Optimization of acquisition and processing times for the measurement of 1H to 13C polarization transfer kinetics

Xavier Falourd, Marc Lahaye, Corinne C. Rondeau-Mouro

MethodsX 9 (2022) 101914

Contents lists available at ScienceDirect

MethodsX

journal homepage: www.elsevier.com/locate/mex

Method Article

Optimization of acquisition and processing times for the measurement of ^{1}H to ^{13}C polarization transfer kinetics

X. Falourd [a,c,*], M. Lahaye [a], C. Rondeau-Mouro [b]

[a] INRAE, UR1268 BIA, F-44316, Nantes, France
[b] INRAE, UR1466 OPAALE, 17 Avenue de Cucillé, CS 64427, F-35044 Rennes, France
[c] INRAE, BIBS Facility, F-44316, Nantes, France

A B S T R A C T

Solid-state NMR (ssNMR) is a unique technique allowing the study of macromolecular assemblies in their native state without prior modification. The proposed method simplifies the current long and tedious data-acquisition and processing protocols for Variable Contact Time (VCT) ssNMR experiments used in dynamic studies of macromolecular assemblies. Using cellulose nanocrystals as a model for polysaccharide assembly, the acquisition time was reduced by decreasing the number of scans and shortening the recycling time required for the ^{1}H to ^{13}C polarization transfers.

- A tenfold reduction in the acquisition time for each kinetic point was achieved while maintaining a good signal to noise ratio.
- The processing time for the pseudo-2D solid-state NMR data was also shortened by using signal intensities derived from peak picking rather than the classically-used spectral deconvolution method.
- These optimizations enabled the molecular dynamic parameters $T_{1\rho}{}^{H}$, T_{HH}, T_{CH} to be accessed within a day.

A R T I C L E I N F O
Method name: Variable Contact Time-Cross Polarization Magic Angle Spinning (VCTCPMAS)
Keywords: Solid-state NMR, VCT-CPMAS, Cellulose
Article history: Received 23 January 2022; Accepted 30 October 2022; Available online 9 November 2022

* Corresponding author.
E-mail address: xavier.falourd@inrae.fr (X. Falourd).

https://doi.org/10.1016/j.mex.2022.101914

Specifications table

Subject Area:	Chemistry
More specific subject area:	*Organization and dynamics of macromolecular assemblies*
Method name:	*Variable Contact Time-Cross Polarization Magic Angle Spinning (VCT-CPMAS)*
Name and reference of original method:	*Müller, L., Kumar, A., Baumann, T., & Ernst, R. R. (1974). Transient oscillations in NMR cross-polarization experiments in solids. Physical Review Letters, 32(25), 1402.* *Hjertberg, T., Zadorecki, P., & Arwidsson, M. (1986). Characterization of cellulose ethers by ^{13}C NMR, 1. Studies of high molecular weight polymers in solution and in the solid state. Die Makromolekulare Chemie: Macromolecular Chemistry and Physics, 187(4), 899-911.* *Lahaye, M., Falourd, X., Laillet, B., & Le Gall, S. (2020). Cellulose, pectin and water in cell walls determine apple flesh viscoelastic mechanical properties. Carbohydrate polymers, 232, 115768.*
Resource availability:	*Topspin 3.6.2, Peakfit®, Excel®*

Background

Since the introduction of NMR spectroscopy in the 1950s, numerous developments have greatly expanded its use. Nowadays, solid-state Nuclear Magnetic Resonance spectroscopy (ssNMR), has become a major tool in the study of macromolecular assemblies.

This is a particularly attractive technique that requires no or limited sample preparation, thus allowing the properties of the macromolecular assemblies to be studied in their natural state.

In particular, it allows access to dynamic parameters via measurement of relaxation times (e.g. T_1, T_2 or $T_{1\rho}$ [1]), probing the nuclei's environment at scales from micrometers to nanometers. These data are particularly useful for characterizing non-covalent water-biopolymer and biopolymer-biopolymer interactions. In the case of $T_{1\rho}{}^{H}$, the relaxation times provide information on molecular ordering for domain sizes between 2 and 30 nm [3]. These measurements require complex pseudo-2D NMR sequences such as the VCT-CPMAS method (Variable Contact Time-Cross Polarization Magic Angle Spinning) [2] which is classically used. This experiment consists in the application of a radiofrequency pulse to the protons, which then fulfil what is known as the Hartmann-Hahn condition (matched nutation frequencies for ^{1}H and ^{13}C) for a given time (contact time CT) during which cross-polarization (CP) occurs (Fig. 1a) [4]. As CT increases, the polarization of the carbons increases until it reaches a maximum. It then decreases as it dissipates into the network during longer CTs (Fig. 1b). The rate of polarization transfer is related to the strength of the dipolar interactions: the stronger they are, the faster the transfer. To extract the dynamic parameters, mathematical modelling of the curve construction is required by plotting signal intensity as a function of CT [5]. It thus requires a sufficient number of points to be registered; the greater the number, the better the fit. Building this curve is time consuming with very long acquisition times. It is therefore important to optimize data-acquisition conditions to increase the number of kinetic points registered within

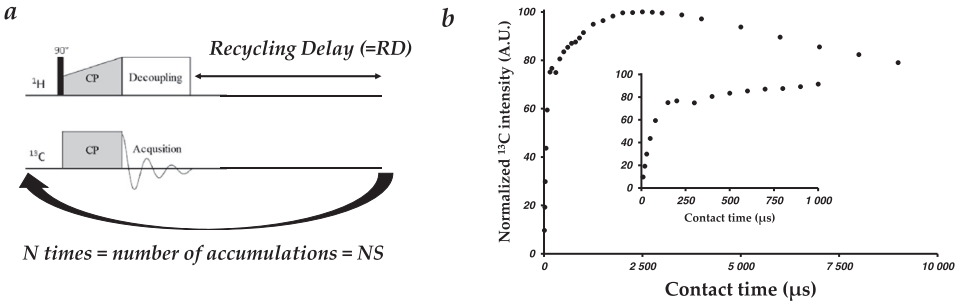

Fig. 1. (a) The CPMAS sequence. (b) Experimental data from ^{1}H-^{13}C transfer kinetics with 30 contact times.

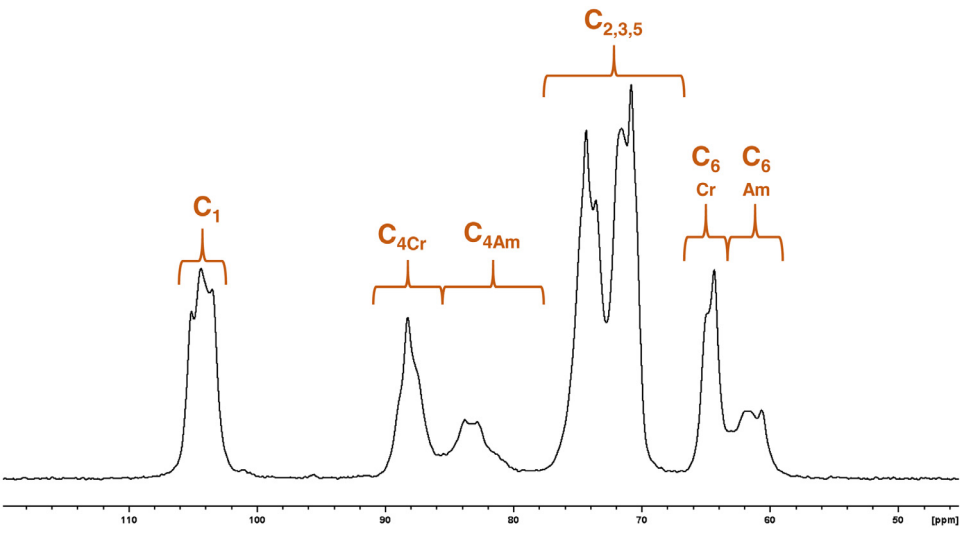

Fig. 2. ^{13}C CPMAS NMR spectrum for cotton nanocrystals with annotations showing chemical shifts associated with carbons in the glucose (Cr=crystalline, Am=amorphous).

a reasonable time. Furthermore, the processing of ssNMR data is quite laborious. The low resolution levels of ssNMR spectra require spectral deconvolution to determine the area proportions of various overlapping signals. Such processing involves data extraction and treatment using dedicated software programmes and this step is also time consuming.

From the first studies performed in the 1970s [6], VCT-CPMAS experiments have always been carried out using a low number of kinetic points, which has led to insufficient attention to the complexity of the rising part of the kinetics curve [7]. This limitation continues to cause difficulties in modelling these data in a satisfactory manner [8]. The present work proposes a procedure using cellulose nanocrystals as models of a macromolecular assembly that aims to optimize the acquisition and processing times necessary to extract kinetic parameters from the classical VCT-CPMAS experiment. Acquisition times were minimized by reducing the number of scans and recycling times without impacting the reliability of the information. The signal-intensity measurement methods for each contact time were studied by comparison between the long spectral decomposition approach and a quicker peak-picking procedure. The whole optimization pipeline proposed here will be applicable to any type of sample providing that appropriate validation of the acquisition and processing parameters is carried out. A kinetic of 30 points, 512 accumulations and 8 seconds of recycling delay was chosen as the reference on the basis of previous work [7,8].

Experimental design

ssNMR spectra were registered on a Bruker Advance III 400 spectrometer at a proton frequency of 400.13 MHz and a carbon frequency of 100.62 MHz. A double resonance $^{1}H/X$ CPMAS 4 mm probe coupled with a high power-level amplifier was used for the ^{13}C CPMAS experiment. The magic angle spinning (MAS) rate was set at 12 kHz and each acquisition was acquired at ambient temperature (298 K). The experiment was conducted using a 90 ° proton pulse of 2.5 µs.

Cotton cellulose nanocrystals (CNC) from the laboratory collection were obtained according to [9]. The acquisitions were carried out on two different rotors, in order to obtain a biological repeat. A typical ^{13}C CPMAS NMR spectrum for CNC is shown in Fig. 2; chemical shifts in the different carbons agree with cellulose I [10]. The areas / intensities obtained were normalized by fixing the maximum value obtained for each kinetic at 100.

Table 1
Number of scans (NS), recycle delay (RD) and associated acquisition durations.

NS	RD (seconds)	duration (minutes)
512	8	68
	6	51
	3	26
	2	17
	1	9
128	8	17
	6	13
	3	6
	2	4
	1	2
64	8	9
	6	6
	3	3
	2	2
	1	1

The ^{1}H to ^{13}C polarization transfer was measured using the VCT-CPMAS sequence shown in Fig. 1a. A cross-polarization ramp (Ramp-CP, from 50% to 100% in steps of 0.5%) was used to avoid mismatches caused by the occurrence of a MAS frequency and dipolar coupling of the same order during acquisition [11].

Thirty contact times were used to validate the acquisition and processing parameters (Fig. 1b). The number of scans (NS) and the recycling delay (RD) (Fig. 1a), were modulated to assess possible time savings during data acquisition (Table 1).

The impact of the processing method on the quality of the results was evaluated. For spectral deconvolution (SD), the chemical shifts, half width and area of ^{13}C peaks were determined using a least-square fitting method with Peakfit® software (Systat software Inc., USA). Peak picking (PP) was carried out using the tool included in the Topspin 3.6.1 acquisition and processing software (BrukerTM) to provide the intensity of each peak.

In order to assess the effect of acquisition and processing parameters on signal intensity, the kinetics were modelled using the I-I*-S model also known as the "two-reservoir" model with isotropic spin diffusion ([5,12,13]). This model is described by the following equation:

$$I(\tau)=I_0 e^{-\tau/T_{1\rho}{}^{H}}\left(1-\lambda e^{-\tau/T_{HH}}-(1-\lambda)e^{-3\tau/2T_{HH}}\times e^{-\tau^2/2T^2_{CH}}\right)$$

Where $I(\tau)$ is the area or the intensity of carbon peak according to the contact time τ, I_0 is the maximum carbon signal area or intensity (associated with the optimal CT), λ is a parameter that depends on the number of protons (n) in the carbons ($\lambda=1/(n+1)$), $1/T_{CH}$ is the mean dipolar coupling between covalently-bonded carbons and protons expressed in hertz, T_{HH} is the spin diffusion time between the two proton reservoirs expressed in seconds, $T_{1\rho}{}^{H}$ is the rotating-frame spin–lattice relaxation time expressed in seconds.

Five parameters were considered: value of the error function ('residue'), T_{CH}, λ, T_{HH} and $T_{1\rho}{}^{H}$. The residue was obtained as follows:

$$R=\sum_{i=1}^{n}[\mathrm{I}model_i - l\exp i]^2$$

Where I_{expi} corresponds to the intensity of the experimental signal for kinetic point number i, and I_{modeli} corresponds to the intensity of the signal determined by modeling for kinetic point number i comprising n points [2].

Fig. 3 shows the fitting of the experimental data points in relation to contact times in order to estimate the dynamic parameters for the signal variations.

The distribution of the resulting values was represented on boxplots (Figs. 6–11) and a Student's t-test preceded by a Fisher test were used to check for the homoscedasticity of the results. The

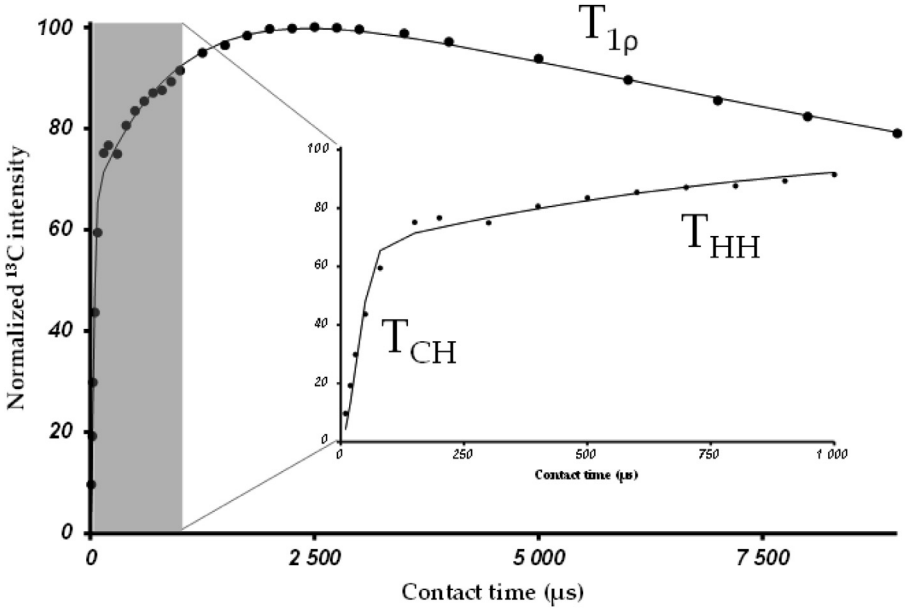

Fig. 3. Representation of the experimental data (dots) and fitted model (black line).

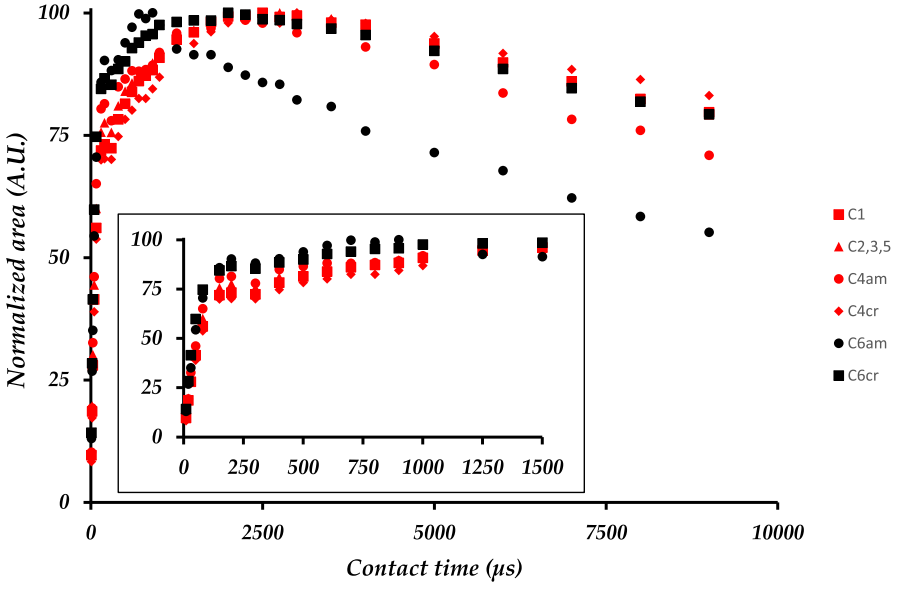

Fig. 4. Normalized area of each CNC carbon relative to contact time. The insert shows the signal evolution for short contact times (< 1500 µs). These data were obtained with 512 accumulations and recycling delays of 8 s.

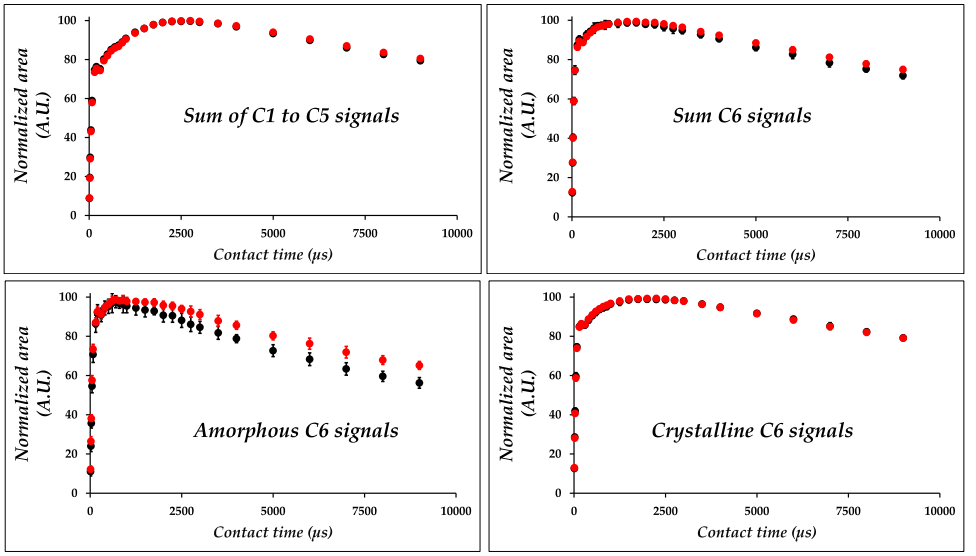

Fig. 5. Normalized area (black) and intensity (red) with standard deviations (vertical lines) for the different kinetics used in this study (n=20).

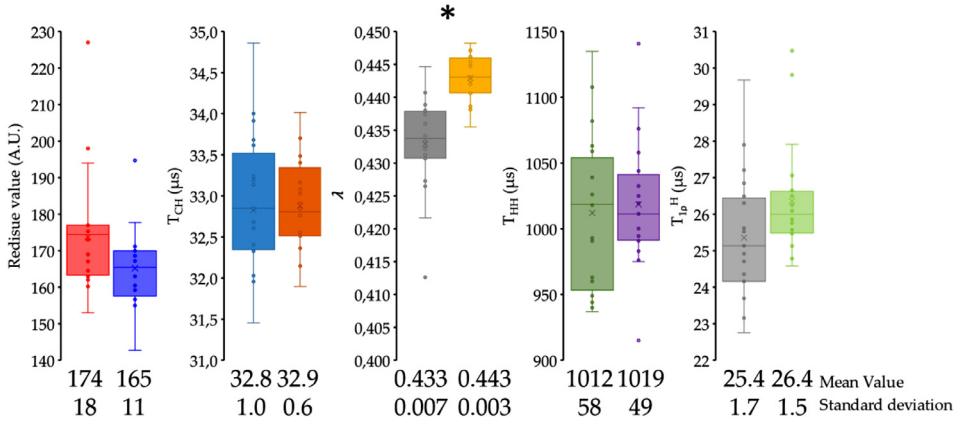

Fig. 6. Boxplots of the values obtained by modelling the sum of signals C1 to C5 calculated using SD (left) and PP (right) for the values of the residues, T_{CH}, λ, T_{HH} and $T_{1\rho}^{H}$. *: significant difference (p:000001).

threshold for significant differences was $p < 0.05$. Statistics were realized using Excel software (Microsoft). Data with 512 and 128 accumulations were selected as repetitions for the evaluation of the processing method (2 samples, 5 RD and 2 NS, giving 20 repetitions). Data with 512, 128 and 64 accumulations processed using the PP method were selected as repetitions for the evaluation of the duration of RD (15 repetitions). Data with five recycling delays processed using the PP method were used as repetitions for the evaluation of the number of scans (10 repetitions).

For practical reasons, the processing parameters were optimized first followed by optimization of the acquisition parameters. Indeed, given the time-consuming nature of spectral deconvolution, validation of peak picking was a critical step.

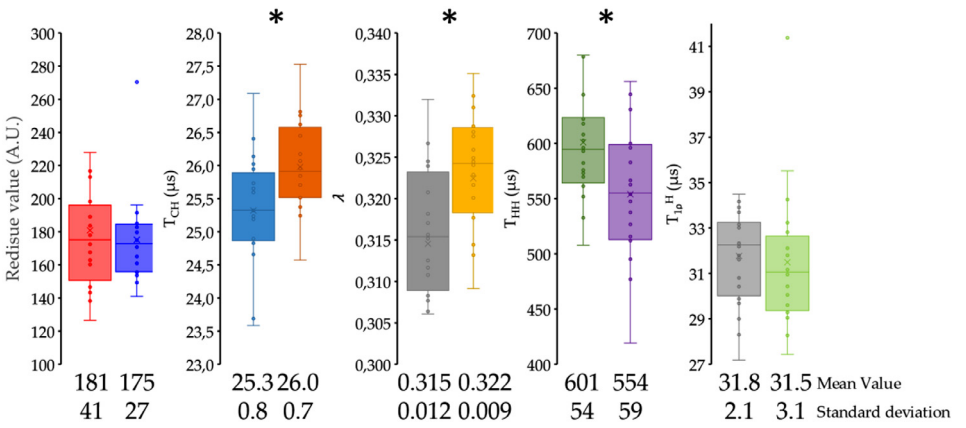

Fig. 7. Boxplots of the values obtained by modelling the areas/intensities of crystalline C6 calculated using SD (left) and PP (right) for the values of the residues, T_{CH}, λ, T_{HH} and $T_{1\rho}{}^{H}$. *: significant difference (p=0.01 for T_{CH}, 0.02 for λ and 0.01 for T_{HH}).

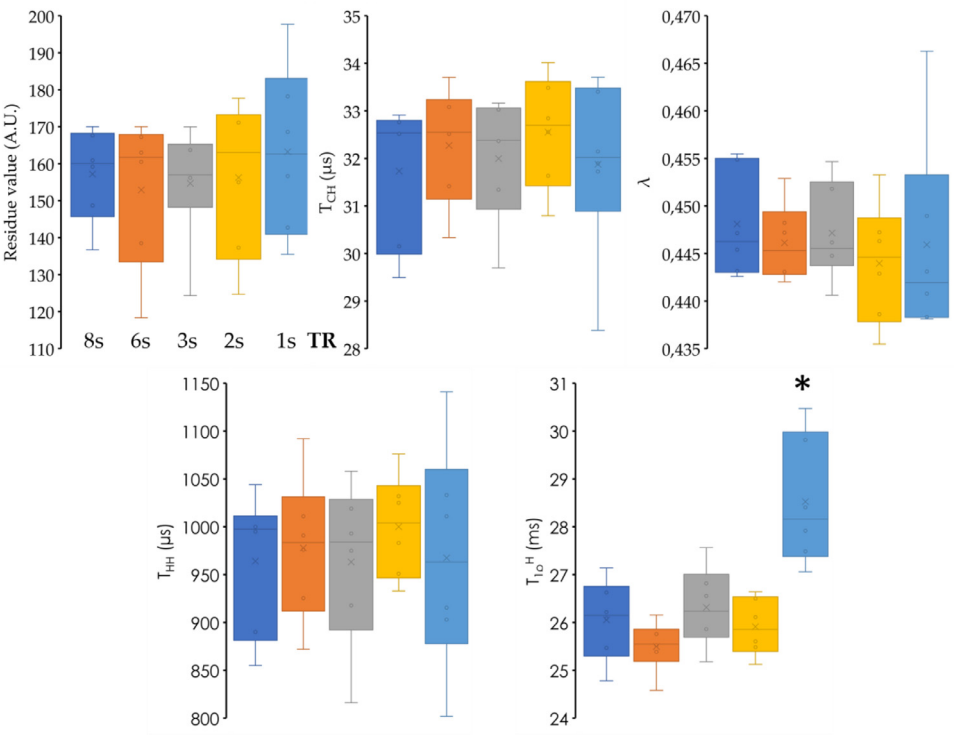

Fig. 8. Boxplots of the values obtained by modelling the sum of C1 to C5 intensities calculated using PP for the values of the residues, T_{CH}, λ, T_{HH} and $T_{1\rho}{}^{H}$ as a function of the recycling delay. *: significant difference (p<0.01 for $T_{1\rho}{}^{H}$ with 1 second RD compared to the other 4).

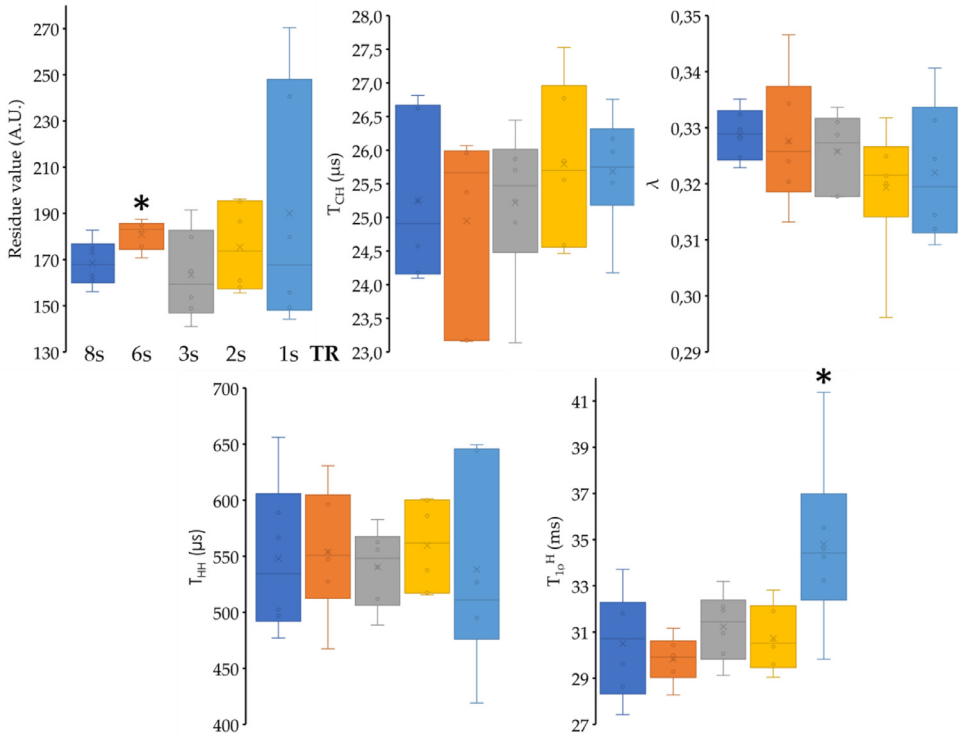

Fig. 9. Boxplots of the values obtained by modelling the crystalline C6 intensities calculated using PP for the values of the residues, T_{CH}, λ, T_{HH} and $T_{1\rho}{}^{H}$ as a function of the recycling delay. *: significant difference (p=0.03 for residue values between 8 and 6 seconds, p<0.01 for $T_{1\rho}{}^{H}$ with 1 second RD compared to the other 4).

Validation of the peak picking processing method

In solid-state NMR spectra, the frequent overlapping peaks require spectral deconvolution to access chemical shift values and signal measurements (area, intensity). When tracking ^{1}H to ^{13}C cross-polarization, each ^{13}C peak characterized by a chemical shift, a width at half height and a shape (Lorentzian / Gaussian distribution) evolves over time as its intensity and area change. As the first three parameters do not change as a function of contact time, the PP method was assessed as an alternative to SD. This evaluation is also based on the fact that the overlapping CNC carbons are expected to have similar kinetics. The comparison of the two processing methods (SD or PP) was based on a boxplot representation and, using the means, on standard deviations and the results of Fisher and Student tests.

As shown in Fig. 4 (NS = 512, RD = 8 s), the signal kinetics for C1 to C5 (in red) have similar behaviors, especially in the rising part of the kinetic curve. For C6, despite a large difference between the crystalline and amorphous signals for long contact times, the signals are similar for short contact times. For all these reasons, signals C1 to C5 were grouped in a first pool, by summing the areas/intensities obtained for C1, amorphous C4, crystalline C4 and C2,3,5.

The C6 signals were grouped in a second pool by summing the areas/intensities obtained for amorphous C6 and crystalline C6. In order to validate this second grouping, which had no obvious cause, the amorphous and crystalline C6 signals were also processed separately. It was confirmed that, despite similar behaviors up to a CT of 1 ms, these kinetics did indeed diverge somewhat thereafter. In addition, as shown in Fig. 2, the spectral resolution of amorphous C6 is lower than that of crystalline C6, which can lead to a larger dispersion values.

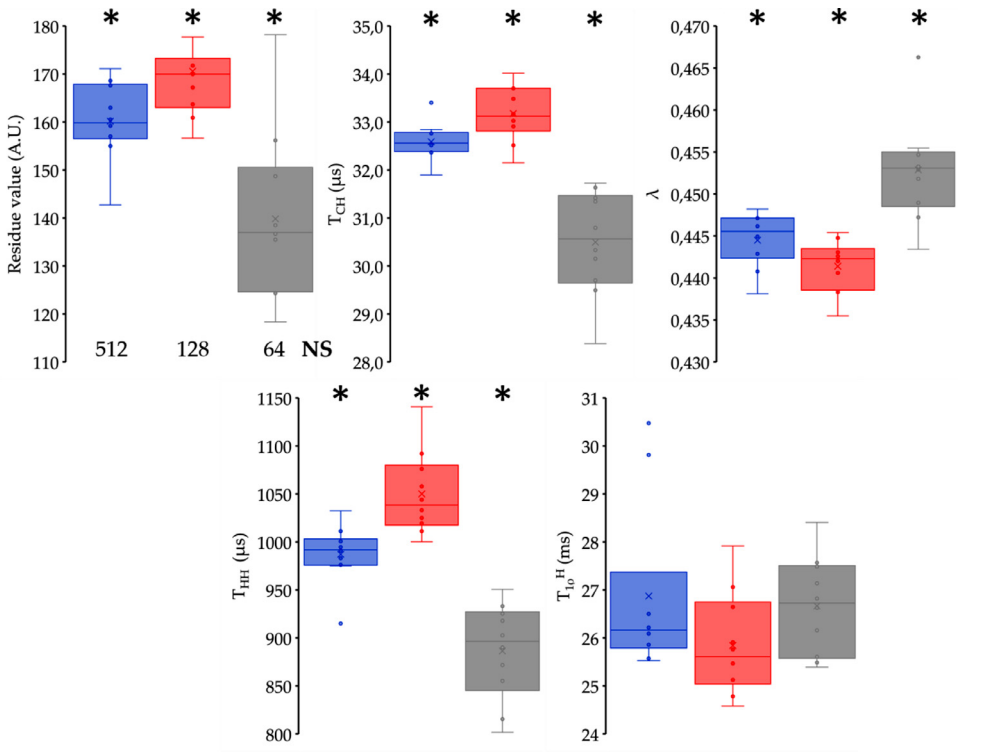

Fig. 10. Boxplots of the values obtained by modelling the sum of the C1 to C5 intensities calculated using PP for the values of the residues, T_{CH}, λ, T_{HH} and $T_{1\rho}{}^{H}$ as a function of the number of accumulations. *: significant difference ($p<0.01$ for all data marked with an asterisk).

The dispersion of the experimental values (n=20) for the differing kinetic signals is shown in Fig. 5. The dispersion of kinetic values obtained by summing the values of C1 to C5 is very low (mean standard deviation=0.67). The kinetics obtained by summing the C6 values show greater dispersion (mean standard deviation=1.46), which is mostly due to the standard deviation of the amorphous C6 signals (mean standard deviation=2.74). For this reason, the C6 kinetics have been studied using only crystalline C6 data.

As shown in Fig. 6, no difference between the results of SD and PP methods on C1 to C5 signals was observed, except for the λ value ($p=0.00001$). This difference between the mean values is, however, very small and does not leave room for differences in interpretation [5]. As peak picking is more than ten times faster than spectral deconvolution, it was the method chosen for the remainder of the work. It should be noted that this method is possible because CNC is a pure cellulose compound. For more complex compounds such as cell-wall or lignocellulosic biomasses, the peaks of other compounds (hemicelluloses and/or lignins) could overlap with cellulose signals. In such cases, PP could therefore produce different results compared with SD. It is interesting to note that the calculated value of λ (0.44) is lower than the theoretical value (0.5 for a CH). It is therefore possible that the relationship could be influenced by other factors, thus requiring a separate study.

The values for the crystalline C6 are more dispersed than for the pooled C1-C5 (Fig. 7) and led to a significant difference in T_{CH} ($p=0.01$), λ ($p=0.02$) and T_{HH} ($p=0.01$) values. It was observed that the modelling used, although appropriate for the kinetics of C1-C5, was not suitable for the C6. Indeed, it is necessary for $T_{1\rho}{}^{H}$ values to be similar, independently of the carbon used. Because C6 are CH_2 groups and C1 to C5 are CH groups, they have different dynamics. Nevertheless, there is still interest

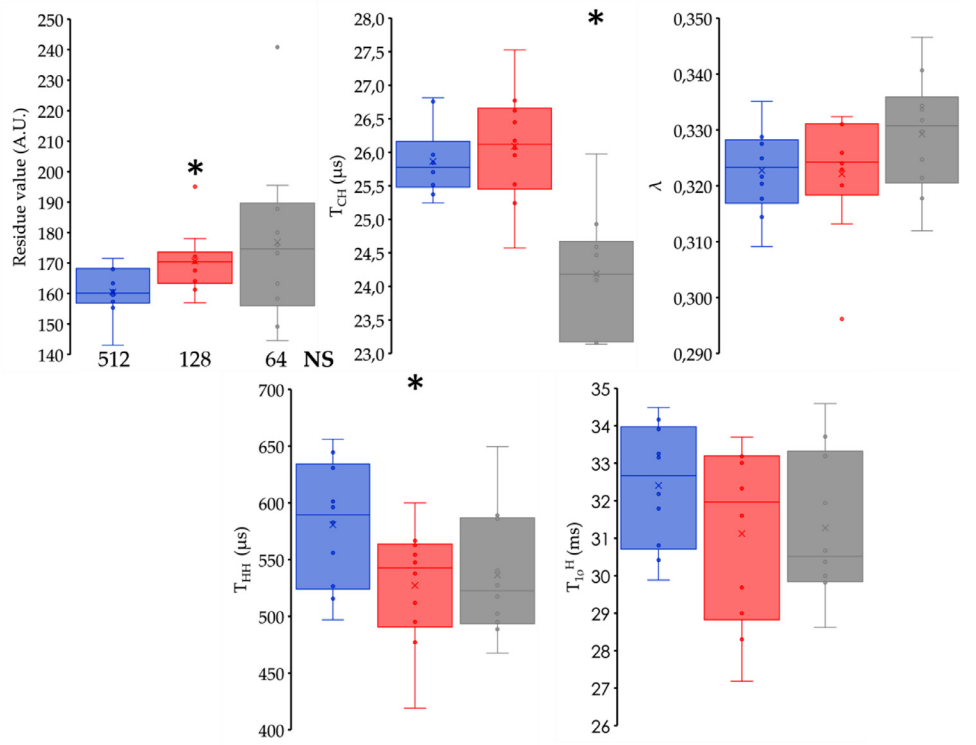

Fig. 11. Boxplots of the values obtained by modelling the crystalline C6 intensities calculated using PP for the values of the residues, T_{CH}, λ, T_{HH} and $T_{1\rho}{}^{H}$ as a function of the number of accumulations. *: significant difference ($p<0.01$ for all data marked with an asterisk).

in obtaining information from the crystalline C6. In this case the calculated value of λ (0.32) is close to the theoretical value (0.33 for a CH_2).

Optimization of acquisition parameters

- Recycling delay

RD allows an excited sample to return to its initial energy equilibrium before the next acquisition. Too short a delay produces a non-quantitative signal due to partial saturation. Conventionally, the minimum time required is 5 times the T_1 [14]). In our case, T_1 is equal to at least 1.5 s (data not shown), which would require a RD of 7.5 seconds. However, in the case of a dynamic experiment where ^{1}H magnetization is transferred to ^{13}C, it is not absolutely necessary for the ^{1}H magnetization to return to full equilibrium [15]. Indeed, Nakai (2013) has shown that optimal efficiency in signal acquisition occurs when the recycle delay RD is set at about 1.3 times T_1. Recycling times were therefore reduced in the present study, as shown in Fig. 8. This action had no significant effect on the residue values, T_{CH}, λ or T_{HH}. For $T_{1\rho}{}^{H}$ a RD value of 1 s led to significant variation (Fig. 8). It can thus be concluded that a recycling time of at least 2 s is sufficient in the case of cellulose. This result is valid for the sum of the signals from C1 to C5 and for the crystalline C6 (see Fig. 9). The significant difference ($p=0.03$) in the residue values between 8 and 6 seconds of recycling time for crystalline C6 does not lead to differences in the values obtained in the modelling and therefore does not influence the choice of RD value.

- Number of accumulations

Usually, a large number of scans are accumulated in order to obtain a suitable signal to noise ratio for each data point at each contact time. In order to assess the minimum number of scans necessary, 64, 128 and 512 scans were tested. As can be seen in Fig. 10, surprisingly, the residue decreased strongly for NS = 64. This result may be due to the inadequacy of the kinetics modelling used. Optimally, according to Fig. 10, a minimum of 512 accumulations would be required. However, the difference between both residues and kinetic parameters measured with 512 scans and 128 scans is far less than that between measurements from 128 and 64 scans. In addition to the similarity in residue values, T_{HH} values after 512 scans (987 µs) and 128 scans (1050 µs) are close to the value obtained in the method validation (1015 µs) unlike the value obtained for 64 scans (887 µs). The same observation holds for T_{CH} and λ. Thus, 128 accumulations would appear suitable to obtain reliable kinetic data. As shown in Fig. 11, for crystalline C6, the effect of the number of accumulations is less marked than for the C1 to C5 signals, suggesting that 128 or even 64 accumulations are sufficient if this signal alone is to be used.

Conclusions

The proposed method to optimize the acquisition and processing parameters in VCT ssNMR experiments provides means to achieve marked time-saving in the assessment of dynamic parameters in complex polysaccharide assemblies. Using cellulose nanocrystals as a model, spectra acquisition can be performed with 128 accumulations and a recycling delay of 2 seconds. Only the crystalline C6 signals must be studied due to the difficulty in processing the signal that corresponds to the amorphous phase. These conditions allow acquisition of a classical kinetic curve made up of 30 contact times in approximately 2 h instead of the 34 h required for the usual settings (NS=512 and RD=8 seconds). Peak picking as an alternative to peak deconvolution is a major contributor to the time saving of the whole process. In fact, for kinetics constructed using 30 contact times, spectral deconvolution takes approximately 3 h, while peak picking takes only about 20 min. It is now possible to include either a larger number of samples or a higher number of contact times enabling detailed kinetic curves to be built for complex model fitting with more appropriate equations. However, it is important to emphasize that the acquisition parameters and processing method are substrate-dependent and must be optimized and validated for other complex systems. This method provides a general framework with parameters that are likely to be usable as starting parameters for the optimization of similar ssNMR experiments on other complex polysaccharide assemblies, such as lignocellulosic materials. For such heterogeneous materials, it will probably be necessary to identify one or more characteristic signals where the line overlap does not include molecules with contrasting dynamics.

Declaration of Competing Interest

The authors declare that they have no known competing financial interests or personal relationships that could have appeared to influence the work reported in this paper.

Data Availability

Data will be made available on request.

Acknowledgments

The authors thank Isabelle Capron (UR BIA, INRAE) for providing the CNC. Solid state NMR experiments were performed at the BIBS facility (UR1268 BIA, IBiSA, Phenome-Emphasis-FR (grant number ANR-11-INBS-0012)).

References

[1] D.C. Apperley, R.K. Harris, Hodgkinson P, Solid-state NMR: Basic principles and practice, Momentum Press, 2012, doi:10.5643/9781606503522.

[2] R.J. Smernik, J.A. Baldock, J.M. Oades, A.K. Whittaker, Determination of T1ρH relaxation rates in charred and uncharred wood and consequences for NMR quantitation, Solid State Nucl. Magn. Reson. (2002), doi:10.1006/snmr.2002.0064.

[3] R.H. Newman, Nuclear magnetic resonance study of spatial relationships between chemical components in wood cell walls, Holzforschung (1992), doi:10.1515/hfsg.1992.46.3.205.

[4] S.R. Hartmann, E.L. Hahn, Nuclear double resonance in the rotating frame, Phys. Rev. (1962), doi:10.1103/PhysRev.128.2042.

[5] W. Kolodziejski, J. Klinowski, Kinetics of cross-polarization in solid-state NMR: a guide for chemists, Chem. Rev. (2002), doi:10.1021/cr000060n.

[6] L. Müller, A. Kumar, T. Baumann, R.R. Ernst, Transient oscillations in NMR cross-polarization experiments in solids, Phys. Rev. Lett. (1974) /10.1016%2Fj.jmr.2014.10.013.

[7] T. Hjertberg, P. Zadorecki, M. Arwidsson, Characterization of cellulose ethers by 13C NMR, 1. Studies of high molecular weight polymers in solution and in the solid state. Die Makromolekulare Chemie: Macromolecular Chemistry and Physics, 1986, doi:10.1002/macp.1986.021870419.

[8] M. Lahaye, X. Falourd, B. Laillet, S. Le Gall, Cellulose, pectin and water in cell walls determine apple flesh viscoelastic mechanical properties, Carbohydrate polymers, 2020, doi:10.1016/j.carbpol.2019.115768.

[9] C.J. Saelices, M. Save, I. Capron, Synthesis of latex stabilized by unmodified cellulose nanocrystals: the effect of monomers on particle size, Polym. Chem. (2019), doi:10.1039/C8PY01575A.

[10] R.H. Newman, T.C. Davidson, Molecular conformations at the cellulose–water interface, Cellulose (2004) 10.1023/B%3ACELL.0000014778.49291.C6.

[11] G. Metz, X.L. Wu, S.O. Smith, Ramped-amplitude cross polarization in magic-angle-spinning NMR, J. Magn. Reson. (1994) Series A, doi:10.1006/jmra.1994.1208.

[12] M. Paris, H. Bizot, J. Emery, J.Y. Buzare, A. Buleon, NMR local range investigations in amorphous starchy substrates: II-Dynamical heterogeneity probed by 1H/13C magnetization transfer and 2D WISE solid state NMR, Int. J. Biol. Macromol. (2001), doi:10.1016/S0141-8130(01)00161-1.

[13] L. Dagys, V. Klimavicius, T. Gutmann, G. Buntkowsky, V. Balevicius, Quasi-equilibria and polarization transfer between adjacent and remote spins: 1H–13C CP MAS kinetics in glycine, J. Phys. Chem. A (2018), doi:10.1021/acs.jpca.8b09036.

[14] A. Abragam, The Principles of Nuclear Magnetism, Oxford University Press, 1961, doi:10.1063/1.3057238.

[15] T. Nakai, Solid-state 29Si NMR for Evaluating Microscopic Sites of Glass Materials: 29Si Measurements in Multinuclear NMR, Most Efficient Measurements, Quantitative Measurements, Advanced Measurements, New Glass, 2013.